Kinetic Study on Vibrational Relaxation of SO($B^3\Sigma^-$, $v' = 1$ and 2) by Collisions with He

Katsuyoshi Yamasaki,* Fumikazu Taketani, Yuichi Takasago, Kazuyuki Sugiura, and Ikuo Tokue

Department of Chemistry, Niigata University, Ikarashi, Niigata 950-2181, Japan

Received: January 23, 2003; In Final Form: April 13, 2003

Rate constants for vibrational relaxation of SO($B^3\Sigma^-$, $v' = 1$ and 2) by collisions with He have been determined. SO($X^3\Sigma^-$) was generated in the photolysis of SO_2 at 193 nm, and excited to a single vibrational level of the $B^3\Sigma^-$ state with a tunable UV laser. Dispersed fluorescence spectra were recorded as a function of buffer gas pressures (He, 30−150 Torr). Observed spectra are composed of fluorescence from the initially excited level and those from levels populated by vibrational relaxation. Kinetic analyses of relative fluorescence intensities give rate constants for both single- and double- quantum vibrational relaxation: $(7.7 \pm 1.0) \times 10^{-13}$ for $v' = 1 \rightarrow v' = 0$, $(1.0 \pm 0.2) \times 10^{-11}$ for $v' = 2 \rightarrow v' = 1$, and $(1.7 \pm 0.3) \times 10^{-12}$ for $v' = 2 \rightarrow v' = 0$, in units of cm^3 $molecule^{-1}$ s^{-1} (the quoted errors are 2σ). It has been found that the branching ratios between quenching and vibrational relaxation of SO($A^3\Pi$ and $B^3\Sigma^-$) by monatomic gases are strongly dependent on the number of perturbed rotational levels.

Introduction

The SO radical has been a target as a medium of optically, chemically, or discharge pumped tunable UV laser.[1−6] Miller et al.[6] have succeeded in observing optically pumped lasing via the $B^3\Sigma^- - X^3\Sigma^-$ system. They pumped the 0−2 vibrational band and observed lasing of the $0-v''$ progression ($v'' = 8-11$). The 0−2 band, however, has a very small Franck−Condon factor, 0.00869[7] or 0.007,[8] and pumping to vibrational levels with larger Franck−Condon factors might be more efficient in lasing. When SO is optically pumped to the vibrationally excited levels of the $B^3\Sigma^-$ state, predissociation, quenching, and vibrational relaxation must be taken into account. It is well-known that vibrational levels higher than the $v' = 3$ of $B^3\Sigma^-$ are nonfluorescent because of efficient predissociation to $S(^3P) + O(^3P)$ by way of the $C^3\Pi$ state.[9,10] Vibrational level $v' = 3$ also undergoes predissociation at relatively low rotational levels ($N' > 10$);[10] therefore, $v' = 1$ and 2 are suitable for lasing. Unfortunately, there have been no reports on the kinetics of vibrational relaxation of SO($B^3\Sigma^-$). It is thus the goal of the present study to measure the rate constants for vibrational relaxation of SO($B^3\Sigma^-$, $v' = 1$ and 2), and to clarify the mechanism governing photochemical processes.

Recently, Stuart et al.[11] have reported the overall removal rate constant of SO($B^3\Sigma^-$, $v' = 2$) by He to be $(1.3 \pm 0.3) \times 10^{-10}$ cm^3 $molecule^{-1}$ s^{-1}. They observed time-resolved fluorescence decay of SO($B^3\Sigma^-$, $v' = 2$) as a function of buffer gas pressures ($P_{He} \leq 10$ Torr); however, they did not evaluate the contributions of vibrational relaxation to overall deactivation. In general, vibrational relaxation of electronically excited states with short lifetimes is difficult to observe, because fast radiative and/or nonradiative processes are likely to obscure vibrational relaxation. Furthermore, rate constants for multiquantum relaxation ($\Delta v \geq 2$) are not readily obtained, because single-quantum vibrational relaxation ($\Delta v = 1$) is predominant over multiquantum relaxation and because both types of relaxation always occur simultaneously.

* Corresponding author. Fax: +81-25-262-7530. E-mail: yam@scux.sc.niigata-u.ac.jp.

In the present study, we have observed buffer gas (He) pressure dependence of dispersed fluorescence spectra, and determined rate coefficients for vibrational relaxation of SO($B^3\Sigma^-$, $v' = 1$ and 2) by He. We present, for the first time, evidence that 15% of vibrational relaxation of $v' = 2$ are double-quantum relaxation ($v' = 2 \rightarrow v' = 0$). We also discuss the mechanism of fast quenching and vibrational relaxation of SO($B^3\Sigma^-$) by He.

Experimental Section

An experimental apparatus has been described previously,[12,13] and specific features for the present study are given here. SO_2 (3 mTorr) in a buffer gas (He, ≤150 Torr) was photolyzed at 193 nm with an ArF excimer laser (Lambda Physik LEXtra50, 19 Hz) at 298 ± 2 K, and SO($X^3\Sigma^-$) was generated. Vibrational levels of SO($B^3\Sigma^-$, $v' = 0-2$) were excited via the 0−2, 1−1, and 2−2 bands in the $B^3\Sigma^- - X^3\Sigma^-$ system with a Nd^{3+}:YAG laser (Spectron SL803) pumped frequency doubled dye laser (Lambda Physik LPD3002 with LD489/MeOH and BBO crystal). The line width of the light from the dye laser is $\Delta\tilde{\nu}$(fwhm) = 0.3 cm^{-1}, i.e., 0.002 nm at 250 nm. Time delays between the photolysis (ArF) and excitation (dye) laser were 20 μs in all measurements. Generation of $X^3\Sigma^-$, $v' = 5$ is energetically possible by the excess energy of SO_2 photolysis at 193 nm,[14] and it is well-known that 60−70% of the SO($X^3\Sigma^-$) product is in $v' = 2$.[14−19] It might, therefore, be suggested that excitation to a single vibrational level is disturbed by vibrational cascade in the $X^3\Sigma^-$ state by collisions with bath gases. We have ascertained that none of the three vibrational bands for excitation [0−2 (256.16 nm), 1−1 (245.14 nm), and 2−2 (248.30 nm)] are overlapped with other vibrational bands, and that a single vibrational level can be excited at all pressures and delay times from the photolysis.

The $A^3\Pi - X^3\Sigma^-$ transitions of SO may appear over the nearly identical wavelength range with the $B^3\Sigma^- - X^3\Sigma^-$ system;[1−5,20−30] nevertheless, fluorescence via the $A^3\Pi - X^3\Sigma^-$ system is negligibly weak due to a relatively small effective absorption cross-section $\sigma(A^3\Pi \leftarrow X^3\Sigma^-)/\sigma(B^3\Sigma^- \leftarrow X^3\Sigma^-) = 0.027$.[11] Photoemission from SO_2 is also negligible, because the photoabsorption cross sections of SO_2 at the excitation wavelengths ($\lambda \approx 250$

10.1021/jp034188v CCC: $25.00
Published on Web 05/23/2003

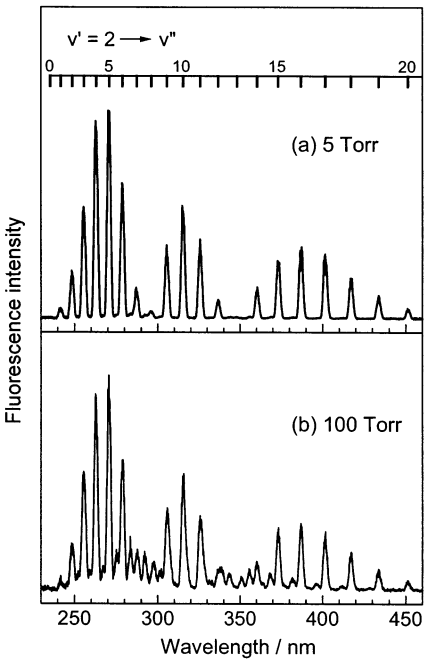

Figure 1. Dispersed fluorescence spectra of the $B^3\Sigma^- - X^3\Sigma^-$ system of SO excited to a single vibrational level ($v' = 2$) at different pressures of a buffer gas (He). The excitation wavelength is 248.30 nm ($R(20)$ of the 2−2 band). $P_{SO_2} = 3$ mTorr, and $P_{total}(He) = 5$ (a) and 100 Torr (b). The delay times between the photolysis (193 nm) and excitation laser are 20 μs. The assignment shown in part a is the transition wavelengths of the $2-v''$ bands. New peaks appearing in part b are fluorescence from $v' = 0$ and 1 populated by vibrational relaxation by collisions with He.

nm), 1×10^{-19} cm^2,[11,31,32] are smaller than that of SO($B^3\Sigma^- \leftarrow X^3\Sigma^-$) by a factor of 2.5×10^4 which more than offsets the concentration ratio $[SO_2]/[SO] \approx 200$ in the present study. Clerbaux and Colin[10] have observed a broad emission, peaking at 350 nm, attributed to the SO + O → SO_2* recombination reaction. The time constant of this reaction is estimated to be ~10 ms under the present experimental conditions, even if the reaction proceeds at the gas kinetic rate, and actually, no emission due to SO + O → SO_2* reaction was observed.

Fluorescence from SO($B^3\Sigma^-$) was collected with a quartz lens ($f = 80$ mm), focused on the entrance slit of a monochromator (JEOL JSG-125S, $f = 125$ cm, $\Delta\lambda$(fwhm) = 3 nm), and detected with a photomultiplier tube (Hamamatsu R928). Signal from the PMT was averaged with a gated integrator (Stanford SR-250), and stored on a disk of a PC after A/D conversion. Wavelength dependence of the sensitivity of photo detection system was calibrated with a superquiet Xe lamp (Hamamatsu L2273).

The flow rates of all the sample gases were controlled with calibrated mass flow controllers (Tylan FC-260KZ and STEC SEC-400 mark3) and mass flow sensors (KOFLOC 3810). Linear flow velocity was 10 cm s^{-1} irrespective of buffer gas pressures. Total pressure (He buffer) was monitored with a capacitance manometer (Baratron 122A). The total pressure measurement together with the mole fractions as measured by the flow controllers gave the partial pressures of the reagents. SO_2 (>99.9%) and He (99.9999%) delivered by Nihon-Sanso were used without further purification. SO_2 was stored in a glass bulb of 3 dm^3 with He (3% dilution).

Results and Analysis

Dispersed Fluorescence Spectra and Buffer Gas Pressure Dependence. Figure 1a shows a dispersed fluorescence from $v' = 2$ of the $B^3\Sigma^-$ state excited via the 2−2 band at 5 Torr of

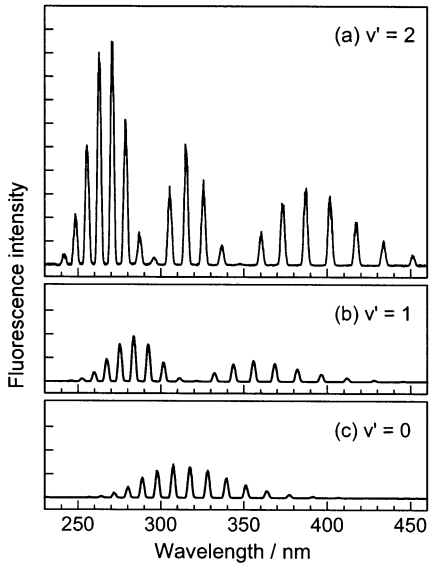

Figure 2. Component fluorescence spectra of the $B^3\Sigma^- - X^3\Sigma^-$ system of SO. The spectra correspond to (a) $A_2(\lambda)$, (b) $A_1(\lambda)$, and (c) $A_0(\lambda)$ in eq 1. The ratios between the intensities of fluorescence from the three levels are calculated from the area of these components: $\int A_2(\lambda)\, d\lambda / \int A_1(\lambda)\, d\lambda / \int A_0(\lambda)\, d\lambda = 0.75/0.14/0.11$.

He buffer gas. All the peaks are assigned to the $2-v''$ bands of the $B^3\Sigma^- - X^3\Sigma^-$ system, and the intensity distributions clearly reflect Franck−Condon factors.[7,8] The wavelengths of vibrational bands were calculated using vibrational constants reported by Clerbaux and Colin.[10] At high buffer gas pressures, new peaks assignable to the $1-v''$ and $0-v''$ bands appear as shown in Figure 1b. Observed dispersed fluorescence spectrum, $A(\lambda)$, following excitation to $v = 2$, consists of fluorescence from $v = 0$, 1, and 2 which are designated by $A_v(\lambda)$:

$$A(\lambda) = A_0(\lambda) + A_1(\lambda) + A_2(\lambda) = c_0 a_0(\lambda) + c_1 a_1(\lambda) + c_2 a_2(\lambda) \quad (1)$$

where $A_v(\lambda) \equiv c_v a_v(\lambda)$ ($v = 0$, 1, and 2), $a_v(\lambda)$ represents the dispersed fluorescence spectrum of a level v recorded at low total pressure (<5 Torr) at which vibrational relaxation hardly occurs, and c_v is the pressure-dependent contribution of $a_v(\lambda)$ to $A(\lambda)$. The factors c_v at a given pressure can be determined from $A_v(\lambda)$ and $a_v(\lambda)$'s by a least-squares analysis using eq 1. Figure 2 shows an example of the components obtained from the spectrum shown in Figure 1b. The sum of the three spectra reproduces the spectrum shown in Figure 1b.

Vibrational Relaxation of SO($B^3\Sigma^-$, $v' = 1$) by He. A kinetic scheme of excited SO($B^3\Sigma^-$, v') in a He buffer gas is as follows:

$$SO(B,v') \xrightarrow{k_{rv'}} SO(X,v'') + h\nu \quad (2)$$

$$SO(B,v') + He \xrightarrow{k_{Qv'}} SO(X) + He \quad \text{or} \quad S + O + He \quad (3)$$

$$SO(B,v') + He \xrightarrow{k_{v',v}} SO(B,v) + He \quad (4)$$

Here $k_{rv'}$, $k_{Qv'}$, and $k_{v',v}$ are rate constants for radiative decay, electronic quenching, and vibrational relaxation, respectively. Quenching is due to deactivation to $X^3\Sigma^-$ and/or predissociation. Rate constants for vibrational up-conversion ($v' < v$) are negligibly small (5%) compared to those for downward relaxation at 298 K, because vibrational quantum energy of $B^3\Sigma^-$ is 620 cm^{-1}.[10,20]

First, consider the case of excitation to $v' = 1$. The rate equation of $v' = 0$ is given as follows:

$$\frac{dN_0^{(1)}(t)}{dt} = k_{10}[He]N_1^{(1)}(t) - (k_{r0} + k_{Q0}[He])N_0^{(1)}(t) \quad (5)$$

Here $N_v^{(v')}(t)$ is the number of molecules in a level v at time t after excitation to a level v'. The intensity of fluorescence from the level v at time t, $I_v^{(v')}(t)$, is related to the population in the level v by $I_v^{(v')}(t) = k_{rv}N_v^{(v')}(t)$. Equation 5 can be written in terms of fluorescence intensities:

$$\frac{dI_0^{(1)}(t)}{dt} = \frac{k_{r0}}{k_{r1}}k_{10}[He]I_1^{(1)}(t) - (k_{r0} + k_{Q0}[He])I_0^{(1)}(t) \quad (6)$$

Integration on both sides of eq 6 from $t = 0$ to ∞ gives

$$I_0^{(1)}(t=\infty) - I_0^{(1)}(t=0) = \frac{k_{r0}}{k_{r1}}k_{10}[He]\int_0^\infty I_1^{(1)}(t)\,dt - (k_{r0} + k_{Q0}[He])\int_0^\infty I_0^{(1)}(t)\,dt \quad (7)$$

There is no population in $v' = 0$ at $t = 0$ or ∞, i.e., $I_0^{(1)}(t = 0) = I_0^{(1)}(t = \infty) = 0$, and consequently, eq 7 leads to the following equation:

$$\frac{k_{r0}}{k_{r1}}k_{10}[He]\int_0^\infty I_1^{(1)}(t)\,dt = (k_{r0} + k_{Q0}[He])\int_0^\infty I_0^{(1)}(t)\,dt \quad (8)$$

When the width of the sampling gate (Δt) is sufficiently larger than that of fluorescence lifetime, then the entire time history of the $B^3\Sigma^-$ state population is collected, and the integrated fluorescence intensities ($\int I_v^{(v')}\,dt$) in eq 8 are in proportion to the areas of component fluorescence $A_v(\lambda)$ (see eq 1):

$$\int_0^\infty I_v^{(v')}\,dt/\Delta t \propto \int_0^\infty A_v(\lambda)\,d\lambda = c_v\int_0^\infty a_v(\lambda)\,d\lambda \equiv S_v^{(v')} \quad (9)$$

The factor c_v has already been obtained by the analysis using eq 1. Δt is fixed to be 100 ns in the present experiments, and is sufficiently larger than the fluorescence lifetimes ($\leq$30 ns) of the $B^3\Sigma^-$ state;[11,13] thus, the following equation is derived from eqs 8 and 9:

$$\frac{S_1^{(1)}}{S_0^{(1)}} = \frac{k_{r1}}{k_{10}}\frac{1}{[He]} + \frac{k_{r1}k_{Q0}}{k_{r0}k_{10}} \quad (10)$$

According to this equation, the slope of the straight line fit from regression analysis of the plot of $S_1^{(1)}/S_0^{(1)}$ against 1/[He] gives k_{r1}/k_{10}. Figure 3a shows the plot of $S_1^{(1)}/S_0^{(1)}$ vs 1/[He]. It should be noted that steeper slopes in Figure 3 give smaller vibrational relaxation rates. We have recently measured the radiative decay rate constant of $v' = 1$ to be $k_{r1} = [3.3 \pm 0.3(2\sigma)]\times10^7$ s^{-1},[13] giving the rate constant for vibrational relaxation $v' = 1 \rightarrow v' = 0$ by He is $k_{10} = [7.7 \pm 1.0(2\sigma)]\times10^{-13}$ cm^3 molecule^{-1} s^{-1}. The error derives mainly from the scatter in the data points of the plots shown in Figure 3 and the confidence level of the radiative decay rate constant. The rate constant k_{10} can also be obtained to be $(1 \pm 0.8) \times 10^{-12}$ cm^3 molecule^{-1} s^{-1} from the intercept of the plot shown in Figure 3a. Unfortunately, the errors of the intercepts are too large ($>\pm$80%) to give k_{10}, and consequently, rate constants of interest have been determined using the slopes.

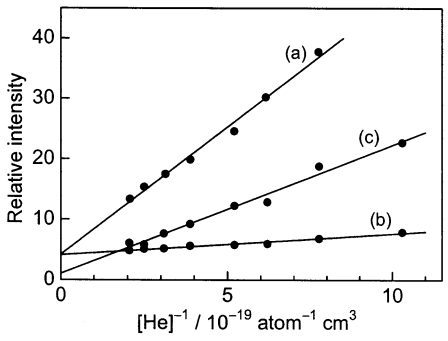

Figure 3. Total pressure dependences of relative fluorescence intensities. The ordinates represent $S_1^{(1)}/S_0^{(1)}$, $S_2^{(2)}/S_1^{(2)}$, and $S_2^{(2)}/(S_0^{(2)} - aS_0^{(1)})$ for parts a−c, respectively (see eqs 10, 11, and 16). The slopes of the straight lines fit from regression analysis correspond to k_{r1}/k_{10}, k_{r2}/k_{21}, and k_{r2}/k_{20} for parts a−c.

Vibrational Relaxation of SO($B^3\Sigma^-$, $v' = 2$) by He. As shown in Figure 1b, fluorescence from $v' = 1$ and $v' = 0$ is observed on excitation to $v' = 2$. There is no doubt that the $v' = 1$ is populated from $v' = 2$ by collisions with He; however, it is not readily concluded how the $v' = 0$ is generated. There are two possible ways to populate the $v' = 0$: one is direct relaxation from $v' = 2$, the other is stepwise relaxation via $v' = 1$. To clarify the relaxation mechanism of $v' = 2$ by He, it is necessary to determine the branching ratios between $v' = 2 \rightarrow v' = 1$ and $v' = 2 \rightarrow v' = 0$.

From the rate equation of $v' = 1$ on excitation to $v' = 2$, the ratios between observed intensities of fluorescence from $v' = 1$ and 2 are derived in the same manner as eq 10:

$$\frac{S_2^{(2)}}{S_1^{(2)}} = \frac{k_{r2}}{k_{21}}\frac{1}{[He]} + \frac{k_{r2}(k_{Q1} + k_{10})}{k_{r1}k_{21}} \quad (11)$$

Figure 3b shows the plot $S_2^{(2)}/S_1^{(2)}$ vs 1/[He], and its slope is k_{r2}/k_{21}. We have measured the radiative decay rate constant of $v' = 2$ to be $[3.7 \pm 0.5(2\sigma)] \times 10^7$ s^{-1},[13] giving $k_{21} = [1.0 \pm 0.2(2\sigma)]\times10^{-11}$ cm^3 molecule^{-1} s^{-1}.

Rate constant for direct relaxation from $v' = 2$ to $v' = 0$ is obtained using the fluorescence intensities of $v' = 0$ on separate excitation to $v' = 1$ and 2. Rate equation for the fluorescence intensity of $v' = 0$ on excitation to $v' = 2$ is given as follows:

$$\frac{dI_0^{(2)}(t)}{dt} = \frac{k_{r0}}{k_{r2}}k_{20}[He]I_2^{(2)}(t) + \frac{k_{r0}}{k_{r1}}k_{10}[He]I_1^{(2)}(t) - (k_{r0} + k_{Q0}[He])I_0^{(2)}(t) \quad (12)$$

Taking account of $I_0^{(2)}(t = 0) = I_0^{(2)}(t = \infty) = 0$ after integration from $t = 0$ to ∞, we obtain

$$\frac{k_{r0}}{k_{r2}}k_{20}[He]S_2^{(2)} + \frac{k_{r0}}{k_{r1}}k_{10}[He]S_1^{(2)} = (k_{r0} + k_{Q0}[He])S_0^{(2)} \quad (13)$$

Note that dispersed fluorescence spectra of $v' = 1$ observed following excitation to $v' = 1$ and 2 at the same buffer gas pressures are identical except for their intensities. A ratio, $S_1^{(2)}/S_1^{(1)} \equiv a$, can be determined from the areas of observed spectra. Equation 8 (or eq 10) gives

$$\frac{k_{r0}}{k_{r1}}k_{10}[He]S_1^{(1)} = (k_{r0} + k_{Q0}[He])S_0^{(1)} \quad (14)$$

and the following expression is obtained from eqs 13 and 14

$$\frac{k_{r0}}{k_{r2}}k_{20}[\mathrm{He}]S_2^{(2)} = (k_{r0} + k_{Q0}[\mathrm{He}])(S_0^{(2)} - aS_0^{(1)}) \quad (15)$$

indicating that $k_{20} \neq 0$ if $S_0^{(2)} \neq aS_0^{(1)}$. Therefore, it can be concluded that double-quantum relaxation $v' = 2 \rightarrow v' = 0$ occurs, if the intensities of fluorescence from $v' = 0$ are different in the spectra in which the intensities of fluorescence from $v' = 1$ on separate excitation to $v' = 1$ and 2 are so scaled to be identical using the factor a. Figure 4, parts a and b, shows dispersed fluorescence spectra recorded on excitation to $v' = 1$ and 2, respectively. The fluorescence from $v' = 1$, 1−12, and 1−13 bands, is adjusted to have identical intensity on excitation to $v' = 1$ and 2. Clearly, fluorescence from $v' = 0$, e.g., the 0−12 band, following excitation to $v' = 2$ is stronger than that on excitation to $v' = 1$ ($aS_0^{(1)} < S_0^{(2)}$), indicating that $k_{20} \neq 0$. This fact is conclusive evidence for the double-quantum vibrational relaxation $v' = 2 \rightarrow v' = 0$ of SO($B^3\Sigma^-$) by He, and is shown for the first time in the present study. The following equation is obtained from eq 15:

$$\frac{S_2^{(2)}}{S_0^{(2)} - aS_0^{(1)}} = \frac{k_{r2}}{k_{20}}\frac{1}{[\mathrm{He}]} + \frac{k_{r2}k_{Q0}}{k_{r0}k_{20}} \quad (16)$$

Figure 3c shows the plot $S_2^{(2)}/(S_0^{(2)} - aS_0^{(1)})$ vs 1/[He], and its slope gives k_{r2}/k_{20}. The rate constant for relaxation $v' = 2 \rightarrow v' = 0$, $k_{20} = [1.7 \pm 0.3(2\sigma)] \times 10^{-12}$ cm^3 molecule^{-1} s^{-1} has been obtained using the radiative decay rate constant of $v' = 2$ measured by the authors.[13]

Discussion

In general, $V-T$ energy transfer by monatomic gases is usually inefficient ($<1 \times 10^{-15}$ cm^3 molecule^{-1} s^{-1}).[33] According to the basic theory for vibrational energy transfer of harmonic oscillator,[34] the probabilities of $V-T$ energy transfer increase linearly with vibrational quantum number v. The selection rule for vibration relaxation of a harmonic oscillator is $\Delta v = 1$, and relaxation with $\Delta v = 2$ is usually small. Rate constants for the vibrational relaxation of SO($B^3\Sigma^-$, $v' = 1$ and 2) by He, measured in the present study, are larger than expected. Also, overall rate constants for relaxation of $v' = 2$, is 15 times larger than that of $v' = 1$, although the vibrational anharmonicity of SO($B^3\Sigma^-$) is small: $\omega_e x_e = 4.79$ cm^{-1} [20] or 2.6 cm^{-1}.[10] Furthermore, 15% of relaxation from $v' = 2$ by He are double-quantum relaxation ($v' = 2 \rightarrow v' = 0$). The extraordinarily large efficiency of vibrational relaxation (particularly of $v' = 2$) can be explained by a large number of nonpredissociating rotational levels perturbed by the $C^3\Pi$ state.

According to the spectroscopic studies,[9,10,35−37] rotational levels in a given vibrational level of the $B^3\Sigma^-$ state are classified into three groups based on the extent of perturbation: low J' levels are unperturbed; some levels of middle J' are perturbed by the $C^3\Pi$ state but do not predissociate; high J' levels predissociate to S(^{3}P) + O(^{3}P) by way of the $C^3\Pi$ state. For the $v' = 0$ of the $B^3\Sigma^-$ state, low J' levels are $J' \lesssim 30$, middle J' levels are $30 \lesssim J' \leq 65$, and high J' levels are $66 \leq J'$; for $v' = 1$, $J' \lesssim 20$ (low J'), $20 \lesssim J' \leq 53$ (middle J'), and $54 \leq J'$ (high J') (Figures 4 and 5 in ref 10). For $v' = 2$, all the levels $J' \leq 37$ belong to middle J', and $38 \leq J'$ are high J'. It should be noted that the $C^3\Pi$ state is not a repulsive electronic state but has a shallow minimum and that not all the levels perturbed by the $C^3\Pi$ state predissociate.[9,10,35] The main process of the low and middle J' levels under collision-free conditions is radiative decay to the $X^3\Sigma^-$ state ($\tau \cong 30$ ns).[11,13] Rotational relaxation by collisions with the bath gases promotes some molecules in the low and middle J' levels to the high J' levels predissociating to S(^{3}P) + O(^{3}P). This is observed as quenching by buffer gases. The probability of $V-T$ energy transfer is usually smaller than the $R-T$ and $V-V$ mechanisms by a few orders of magnitude,[33] and this might be the case for the levels with low J' in the vibrational levels of the $B^3\Sigma^-$ state. Rotational levels with middle J' perturbed by the $C^3\Pi$ state, on the other hand, can couple to other vibrational levels through enhanced interactions via the $C^3\Pi$ state by collisions with bath gases. As described above, all the rotational levels lower than $J' = 38$ of $v' = 2$ are classified as middle J', and the large number of perturbed rotational levels in $v' = 2$ result in the large cross sections for vibrational relaxation.

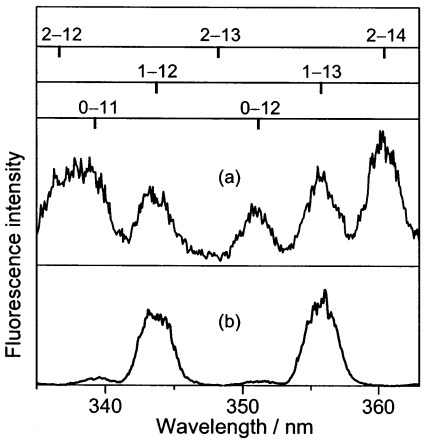

Figure 4. Dispersed fluorescence spectra recorded following excitation to a single vibrational level of SO($B^3\Sigma^-$, $v' = 1$ and 2) along with the assignment of the vibrational bands of the $B^3\Sigma^- - X^3\Sigma^-$ system, with excitation to $v' = 2$ (a) and $v' = 1$ (b). $P_{SO_2} = 3$ mTorr and P_{total}(He) = 100 Torr. Both spectra are so scaled to make the intensities of fluorescence from $v' = 1$ the same. The difference in the intensities of fluorescence from $v' = 0$ gives evidence for the double-quantum vibrational relaxation $v' = 2 \rightarrow v' = 0$.

We have recently measured overall deactivation rate constants of $v' = 1$ and 2 by He to be $(3.9 \pm 0.2) \times 10^{-11}$ and $(1.3 \pm 0.2) \times 10^{-10}$ cm^3 molecule^{-1} s^{-1}, respectively.[13] These are the sum of the rate constants of electronic quenching and vibrational relaxation, and consequently, pure quenching rate constants are $k_{Q1} = (3.8 \pm 0.3) \times 10^{-11}$ for $v' = 1$ and $k_{Q2} = (1.2 \pm 0.2) \times 10^{-10}$ cm^3 molecule^{-1} s^{-1} for $v' = 2$. The contributions of the vibrational relaxation to the overall removal, $f_{relax} = \Sigma_v[k_{v',v}/(k_{v',v} + k_{Qv'})]$, are 0.02 for $v' = 1$ and 0.09 for $v' = 2$. Therefore, vibrational relaxation by He is a minor process compared to electronic quenching. This provides a striking contrast to the case of the $v' = 1$ of SO($A^3\Pi$). McAuliffe et al.[29] have employed a technique similar to the present study, reporting the rate constant for vibrational relaxation of SO($A^3\Pi$, $v' = 1$) by He to be $k_{10}(A) = (4.3 \pm 0.3) \times 10^{-12}$ cm^3 molecule^{-1} s^{-1}. They have also found that the electronic quenching from the $v' = 1$ in the $A^3\Pi$ state by He is negligibly slow, giving an upper limit: $k_{Q1}(A) < (2-3) \times 10^{-13}$ cm^3 molecule^{-1} s^{-1} ($f_{relax} > 0.95$). The large difference in the contributions of vibrational relaxation of $v' = 1$ in the $A^3\Pi$ and $B^3\Sigma^-$ states can be explained by the extent of perturbation.

As stated above, about 15 rotational levels within $20 \lesssim J' \leq 53$ of the $B^3\Sigma^-$, $v' = 1$ are perturbed by the $C^3\Pi$ state. On the other hand, only $J' = 15$ of the $v' = 1$ in $F_2(A^3\Pi_1)$ component is perturbed by the $A'^3\Delta$ state.[24] Therefore, it can be concluded that perturbations increase the probability of quenching more efficiently than relaxation. This propensity can be applied to

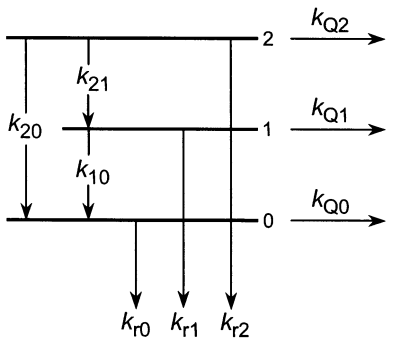

Figure 5. Schematic representation of photochemical processes related to SO($B^3\Sigma^-$, $v' = 0-2$) by collisions with He. Vibrational relaxation: $k_{21} = (1.0 \pm 0.2) \times 10^{-11}$, $k_{10} = (7.7 \pm 1.0) \times 10^{-13}$, and $k_{20} = (1.7 \pm 0.3) \times 10^{-12}$ in units of cm^3 molecule^{-1} s^{-1}. Quenching: $k_{Q0} = (6.3 \pm 0.3) \times 10^{-12}$, $k_{Q1} = (3.8 \pm 0.2) \times 10^{-11}$, and $k_{Q2} = (1.2 \pm 0.2) \times 10^{-10}$ in units of cm^3 molecule^{-1} s^{-1}. Radiative decay: $k_{r0} = (3.5 \pm 0.3) \times 10^7$ s^{-1} (28 ± 2 ns); $k_{r1} = (3.3 \pm 0.3) \times 10^7$ s^{-1} (30 ± 3 ns); $k_{r2} = (3.7 \pm 0.5) \times 10^7$ s^{-1} (27 ± 4 ns). All the quoted errors are 2σ.

other vibrational levels in the $A^3\Pi$ state. McAuliffe et al.[29] have measured quenching rate constant of the $v' = 0$ of $A^3\Pi$ by He to be $k_{Q0}(A) = (4.0 \pm 0.8) \times 10^{-13}$ cm^3 molecule^{-1} s^{-1}, which is close to the $(5.3 \pm 0.9) \times 10^{-13}$ cm^3 molecule^{-1} s^{-1} reported by Lo et al.[5] These rate constants are larger than the upper limit for $v' = 1$ ($k_{Q1}(A) < (2-3) \times 10^{-13}$ cm^3 molecule^{-1} s^{-1}). Stuart et al.[11] have reported the rate constant for quenching of $v' = 5$ in the $A^3\Pi$ state by He to be $k_{Q5}(A) = (4.1 \pm 0.8) \times 10^{-11}$ cm^3 molecule^{-1} s^{-1}. Clyne and Liddy[2] have given no evidence of vibrational relaxation of $v' = 5$ at pressures less than 300 mTorr of various bath gases. Therefore, the efficiency in quenching of the $A^3\Pi$ state by He goes in the order $k_{Q1}(A) < k_{Q0}(A) < k_{Q5}(A)$. Also, quenching of the $A^3\Pi$ state by Ar shows the identical tendency: $(8.5 \pm 1) \times 10^{-13}$ [5] and $(5.1 \pm 1.7) \times 10^{-13}$ [29] for $v' = 0$, $<(3-4) \times 10^{-13}$ for $v' = 1$,[29] and $(7.5 \pm 1) \times 10^{-12}$ for $v' = 5$[29] in units of cm^3 molecule^{-1} s^{-1}. It is surprising that the efficiency in quenching of the $A^3\Pi$ state is not monotonically dependent on v'. Colin and co-workers[10,24] have given evidence that the $A^3\Pi$ state is perturbed at $v' = 0$ and $v' \geq 5$ using the Birge−Sponer analysis, concluding that the levels $v' \geq 5$ are perturbed by the $C^3\Pi$ state. Lo et al.[5] have reported that the $v' = 0$ of $A^3\Pi$ can collisionally couple to a perturbing state $A'^3\Delta$. The strong perturbation occurring on the $v' = 0$ and 5 of the $A^3\Pi$ state accounts for the efficient quenching of $v' = 0$ and 5 of $A^3\Pi$. The findings suggest that collisions with the bath gases enhance the interaction between mutually perturbing levels, resulting in the large probability of quenching even by monatomic gases. Figure 5 shows photochemical processes related to SO($B^3\Sigma^-$, $v' = 0-2$) collisions with He and presents all the rate constants determined by the authors.

Summary

This paper describes vibrational relaxation of SO($B^3\Sigma^-$, $v' = 1$ and 2) by collisions with He. Kinetic analyses of total pressure dependence of relative fluorescence intensity give rate constants for level-to-level vibrational relaxation. We have found the following features: (i) rate constants for vibrational relaxation even by He are extraordinarily large; (ii) relaxation of $v' = 2$ is faster than that of $v' = 1$ by a factor of 15; (iii) 15% of relaxation of $v' = 2$ are due to double-quantum relaxation ($v' = 2 \rightarrow v' = 0$), which is observed for the first time in the present study. These findings are explained by perturbation between the $B^3\Sigma^-$ and $C^3\Pi$ states. The perturbation accelerates quenching more efficiently than vibrational relaxation, which accounts for the small contributions of vibrational relaxation to the overall removal of the $B^3\Sigma^-$ state: $f_{relax} = 0.02$ ($v' = 1$) and 0.09 ($v' = 2$).

Acknowledgment. The authors gratefully acknowledge Craig A. Taatjes (Sandia National Laboratory) for invaluable comments. This work was supported by the Grant-in-Aid for Scientific Research on Priority Areas "Free Radical Science" (Contract No. 05237106), Grant-in-Aid for Scientific Research (B) (Contract No. 08454181), and Grant-in-Aid for Scientific Research (C) (Contract No. 10640486) of the Ministry of Education, Science, Sports, and Culture of Japan.

References and Notes

(1) Clyne, M. A. A.; McDermid, I. S. *J. Chem. Soc., Faraday Trans. 2* **1979**, *75*, 905.
(2) Clyne, M. A. A.; Liddy, J. P. *J. Chem. Soc., Faraday Trans. 2* **1982**, *78*, 1127.
(3) Cao, D.-Z.; Setser, D. W. *Chem. Phys. Lett.* **1985**, *116*, 363.
(4) Cao, D.-Z.; Setser, D. W. *J. Phys. Chem.* **1988**, *92*, 1169.
(5) Lo, G.; Beaman, R.; Setser, D. W. *Chem. Phys. Lett.* **1988**, *149*, 384.
(6) Miller, H. C.; Yamasaki, K.; Smedley, J. E.; Leone, S. R. *Chem. Phys. Lett.* **1991**, *181*, 250.
(7) Smith, W. H.; Liszt, H. S. *J. Quant. Spectrosc. Radiat. Transfer* **1971**, *11*, 45.
(8) Hébert, G. R.; Hodder, R. V. *J. Phys. B* **1974**, *7*, 2244.
(9) Martin, E. V. *Phys. Rev.* **1932**, *41*, 167.
(10) Clerbaux, C.; Colin, R. *J. Mol. Spectrosc.* **1994**, *165*, 334.
(11) Stuart, B. C.; Cameron, S. M.; Powell, H. T. *J. Phys. Chem.* **1994**, *98*, 11499.
(12) Yamasaki, K.; Tanaka, A.; Watanabe, A.; Yokoyama, K.; Tokue, I. *J. Phys. Chem.* **1995**, *99*, 15086.
(13) Yamasaki, K.; Taketani, F.; Tomita, S.; Sugiura, K.; Tokue, I. *J. Phys. Chem. A* **2003**, *107*, 2442.
(14) Kanamori, H.; Butler, J. E.; Kawaguchi, K.; Yamada, C.; Hirota, E. *J. Chem. Phys.* **1985**, *83*, 611.
(15) Kolbe, W. F.; Leskovar, B. *J. Chem. Phys.* **1986**, *85*, 7117.
(16) Kawasaki, M.; Sato, H. *Chem. Phys. Lett.* **1987**, *139*, 585.
(17) Felder, P.; Effenhauser, C. S.; Haas, B.-M.; Huber, J. R. *Chem. Phys. Lett.* **1988**, *148*, 417.
(18) Chen, X.; Asmar, F.; Wang, H.; Weiner, B. R. *J. Phys. Chem.* **1991**, *95*, 6415.
(19) Felder, P.; Haas, B.-M.; Huber, J. R. *Chem. Phys. Lett.* **1993**, *204*, 248.
(20) Herzberg, G. *Molecular Spectra and Molecular Structure, IV. Constants of Diatomic Molecules*; Van Nostrand Reinhold: New York, 1979.
(21) Clyne, M. A. A.; Tennyson, P. H. *J. Chem. Soc., Faraday Trans. 2* **1986**, *82*, 1315.
(22) Smith, W. H. *Astrophys. J.* **1972**, *176*, 265.
(23) Krause, H. F. *Chem. Phys. Lett.* **1981**, *83*, 165.
(24) Colin, R. *J. Chem. Soc., Faraday Trans. 2* **1982**, *78*, 1139.
(25) Wu, K. T.; Morgner, H.; Yencha, A. J. *Chem. Phys.* **1982**, *68*, 285.
(26) Dorthe, G.; Costes, M.; Burdenski, S.; Caille, J.; Caubet, Ph. *Chem. Phys. Lett.* **1983**, *94*, 404.
(27) Johnson, C. A. F.; Kelly, S. D.; Parker, J. E. *J. Chem. Soc., Faraday Trans. 2* **1987**, *83*, 985.
(28) Kulander, K. C. *Chem. Phys. Lett.* **1988**, *149*, 392.
(29) McAuliffe, M. J.; Bohn, M.; Dorko, E. A. *Chem. Phys. Lett.* **1990**, *167*, 27.
(30) Stuart, B. C.; Cameron, S. M.; Powell, H. T. *Chem. Phys. Lett.* **1992**, *191*, 273.
(31) Okabe, H. *Photochemistry of Small Molecules*; Wiley: New York, 1978.
(32) Calvert, J. G.; Pitts, J. N., Jr. *Photochemistry*; John Wiley and Sons: New York, 1966.
(33) Levine, R. D.; Bernstein, R. B. *Molecular Reaction Dynamics and Chemical Reactivity*; Oxford: New York, 1987; Chapter 6.
(34) Yardley, J. T. *Intramolecular Energy Transfer*; Academic Press: New York, 1980.
(35) Colin, R. *Can. J. Phys.* **1969**, *47*, 979.
(36) Abadie, D. *Ann. Phys.* **1970**, *5*, 227.
(37) Klotz, R.; Marian, C. M.; Peyerimhoff, S. D.; Hess, B. A.; Buenker, R. J. *Chem. Phys.* **1983**, *76*, 367.